Supporting Information

Fixing CO_2 from the air to assemble Dy_8 zero-field single-molecule magnets and Gd_8 magnetocaloric molecular materials

Cai-Ming Liu[a,*b], Xiang Hao[a]

[a] *Beijing National Laboratory for Molecular Sciences, CAS Key Laboratory for Organic Solids, Center for Molecular Science, Institute of Chemistry, Chinese Academy of Sciences, Beijing 100190, China*

[b] *School of Chemical Sciences, University of Chinese Academy of Sciences, Beijing 100049, China*

Contents

19. Fig. S13. Magnetic axes of the Dy^{3+} ions in **2** calculated using an electrostatic model

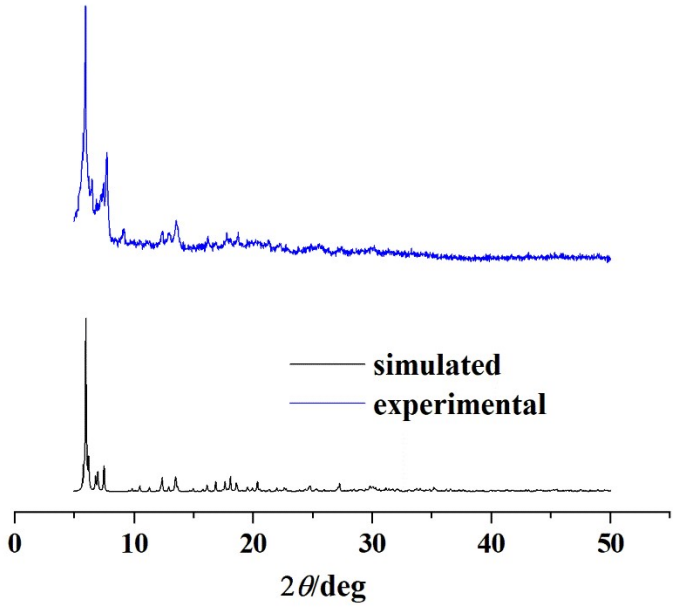

Fig. S1. The simulative and experimental powder X-ray diffraction patterns for **1**.

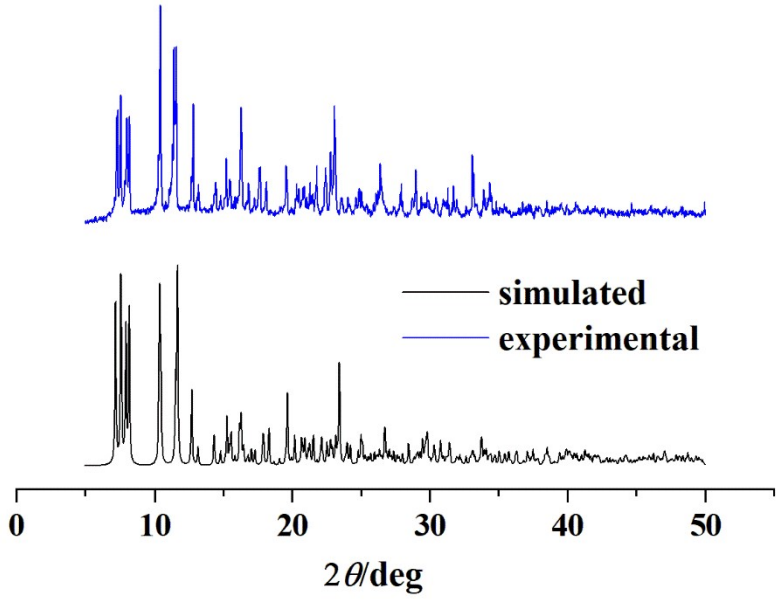

Fig. S2. The simulative and experimental powder X-ray diffraction patterns for **2**.

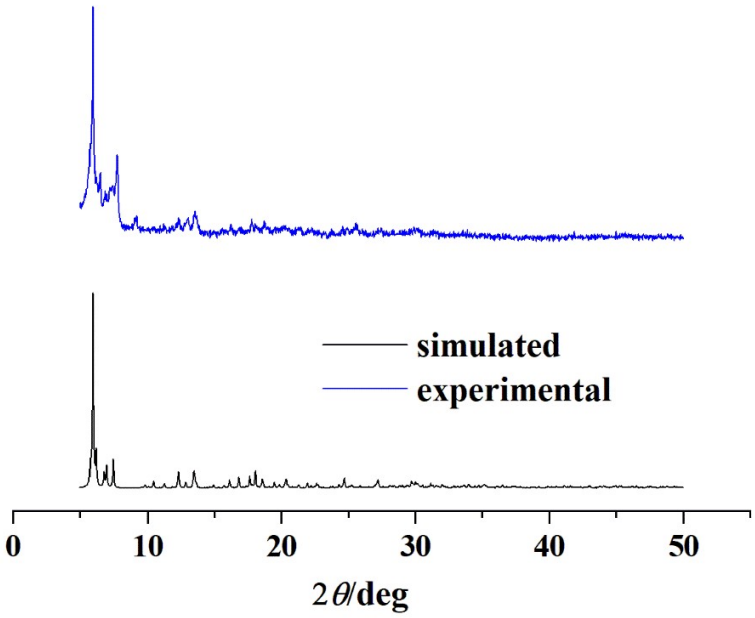

Fig. S3. The simulative and experimental powder X-ray diffraction patterns for **3**.

Table S1. Crystal data and structural refinement parameters for **1**, **2** and **3**.

	1 (squeeze)	**2**	**3** (squeeze)
formula	$C_{124}H_{148}Dy_8N_{44}O_{52}$	$C_{52}H_{84}Dy_2F_6N_{16}O_{22}S_2$	$C_{124}H_{148}Gd_8N_{44}O_{52}$
F_W	4386.85	1788.47	4344.85
crystal system	monoclinic	triclinic	monoclinic
space group	*C*2/*c*	*P*1	*C*2/*c*
a[Å]	32.5183(10)	11.7867(2)	32.5485(8)
b[Å]	18.0719(2)	12.4022(2)	18.1561(4)
c[Å]	31.6045(9)	13.6136(2)	28.8794(8)
α[°]	90.00	65.1480(10)	90.00
β[°]	126.481(4)	87.5400(10)	118.271(3)
γ[°]	90.00	83.2340(10)	90.00
V[Å^3]	14933.6(9)	1793.14(5)	15030.7(7)
Z	4	1	4
ρ_{calc}[g · cm^{-3}]	1.951	1.656	1.920
μ[mm^{-1}]	21.864	12.409	23.277
T[K]	100	100	100
λ [Å]	1.54184	1.54184	1.54184
reflections collected	39305	33926	82338
unique reflections	11047	10359	12462
observed reflections	9334	10233	8652
parameters	912	920	910
GoF[$I \geq 2\sigma(I)$]	1.038	1.020	1.052
R_1[$I \geq 2\sigma(I)$]	0.0457	0.0397	0.0531
$_wR_2$[$I \geq 2\sigma(I)$]	0.1226	0.1040	0.1394
CCDC	2521957	2521958	2521959

Table S2. Selected bond lengths (Å) of **1**, **2** and **3**.

1			
Dy1-N1	2.518(6)	Dy1-N18$^{\#}$	2.675(6)
Dy1-O1W	2.396(6)	Dy1-O2	2.242(5)
Dy1-O3	2.409(5)	Dy1-O12$^{\#}$	2.484(5)
Dy1-O13	2.378(5)	Dy1-O16	2.387(5)
Dy1-O17	2.473(5)	Dy2-N3	2.625(6)
Dy2-N6	2.464(6)	Dy2-O2W	2.346(5)
Dy2-O3	2.363(4)	Dy2-O5	2.212(5)
Dy2-O6	2.369(5)	Dy2-O14	2.296(5)
Dy2 O17	2.327(4)	Dy3 N8	2.653(6)
Dy3-N11	2.515(6)	Dy3-O3W	2.438(5)
Dy3-O6	2.470(5)	Dy3-O8	2.238(4)
Dy3-O9	2.404(5)	Dy3-O14	2.382(5)
Dy3-O15	2.533(5)	Dy3-O18$^{\#}$	2.354(4)
Dy4-N13	2.585(7)	Dy4-N16	2.448(7)
Dy4-O4W	2.379(5)	Dy4-O9	2.358(5)
Dy4-O11	2.235(5)	Dy4-O12	2.339(5)
Dy4-O15	2.290(5)	Dy4-O16$^{\#}$	2.312(4)
2			
Dy1-N1	2.461(7)	Dy1-N8	2.563(7)
Dy1-O1W	2.446(6)	Dy1-O2	2.163(6)
Dy1-O3	2.310(6)	Dy1-O6	2.365(6)
Dy1-O7	2.344(6)	Dy1-O8	2.336(8)
Dy2-N3	2.548(7)	Dy2-N6	2.485(7)
Dy2-O2W	2.335(6)	Dy2-O3	2.369(6)
Dy2-O5	2.163(6)	Dy2-O6	2.327(6)
Dy2-O9	2.399(7)	Dy2-O3W	2.435(6)
3			
Gd1-N1	2.539(7)	Gd1-N8$^{\$}$	2.658(7)
Gd1-O1	2.410(6)	Gd1-O1W	2.466(5)
Gd1-O2	2.272(5)	Gd1-O6$^{\$}$	2.490(6)
Gd1-O13	2.373(5)	Gd1-O16$^{\$}$	2.400(6)
Gd1-O18$^{\$}$	2.580(6)	Gd2-N6	2.505(7)
Gd2-N13	2.639(7)	Gd2-O2W	2.382(6)
Gd2-O5	2.239(6)	Gd2-O6	2.387(6)
Gd2-O9	2.377(5)	Gd2-O14	2.346(5)
Gd2-O16	2.331(5)	Gd3-N11	2.530(8)
Gd3-N18$^{\$}$	2.677(7)	Gd3-O3W	2.412(7)
Gd3-O8	2.263(6)	Gd3-O9	2.430(6)
Gd3-O12$^{\$}$	2.495(6)	Gd3-O14	2.505(5)
Gd3-O15	2.407(5)	Gd3-O17	2.404(6)

Gd4-N3$	2.608(9)	Gd4-N16	2.480(8)
Gd4-O1$	2.378(6)	Gd4-O4W	2.419(6)
Gd4-O11	2.267(6)	Gd4-O12	2.371(6)
Gd4-O15$	2.343(5)	Gd4-O18	2.306(6)

Symmetry codes: #: 1−x, y, 2/3−z; $: 1−x, y, 1/2−z.

Table S3. Dy (III) ion (Dy1 and Dy3) geometry analysis by SHAPE 2.1 software for **1**.

Configuration	ABOXIY **Dy1**	ABOXIY **Dy3**
Enneagon (D_{9h})	32.553	31.781
Octagonal pyramid (C_{8v})	22.094	22.380
Heptagonal bipyramid (D_{7h})	16.222	16.520
Johnson triangular cupola J3 ($C_{3}v$)	13.506	13.614
Capped cube J8 (C_{4v})	6.958	8.025
Spherical-relaxed capped cube (C_{4v})	5.923	6.927
Capped square antiprism J10 (C_{4v})	5.412	4.659
Spherical capped square antiprism (C_{4v})	4.211	3.431
Tricapped trigonal prism J51 (D_{3h})	5.803	5.734
Spherical tricapped trigonal prism (D_{3h})	5.223	4.297
Tridiminished icosahedron J63 (C_{3v})	10.768	10.314
Hula-hoop (C_{2v})	5.183	6.274
Muffin (C_{s})	2.840	2.093

Table S4. Dy (III) ion (Dy2 and Dy4) geometry analysis by SHAPE 2.1 software for **1**.

Configuration	ABOXIY **Dy2**	ABOXIY **Dy4**
Octagon(D_{8h})	29.942	30.045
Heptagonal pyramid(C_{7v})	24.216	24.324
Hexagonal bipyramid(D_{6h})	14.395	14.058
Cube (O_{h})	10.427	9.636
Square antiprism (D_{4d})	2.518	1.969
Triangular dodecahedron (D_{2d})	2.382	2.234
Johnson gyrobifastigium J26 (D_{2d})	12.553	13.126
Johnson elongated triangular bipyramid J14 (D_{3h})	27.114	28.354
Biaugmented trigonal prism J50 (C_{2v})	2.254	2.398
Biaugmented trigonal prism (C_{2v})	1.792	1.914
Snub diphenoid J84 (D_{2d})	3.980	4.185
Triakis tetrahedron (T_{d})	10.944	10.239
Elongated trigonal bipyramid (D_{3h})	23.576	24.092

Table S5. Dy (III) ion geometry analysis by SHAPE 2.1 software for **2**.

Configuration	ABOXIY **Dy1**	ABOXIY **Dy2**
Octagon(D_{8h})	29.604	30.589
Heptagonal pyramid(C_{7v})	23.079	22.198
Hexagonal bipyramid(D_{6h})	16.752	17.420
Cube (O_h)	13.684	13.539
Square antiprism (D_{4d})	3.382	4.311
Triangular dodecahedron (D_{2d})	2.278	2.268
Johnson gyrobifastigium J26 (D_{2d})	13.352	13.192
Johnson elongated triangular bipyramid J14 (D_{3h})	24.630	23.724
Biaugmented trigonal prism J50 (C_{2v})	1.627	2.064
Biaugmented trigonal prism (C_{2v})	1.435	1.816
Snub diphenoid J84 (D_{2d})	3.564	3.277
Triakis tetrahedron (T_d)	14.210	13.954
Elongated trigonal bipyramid (D_{3h})	22.295	21.155

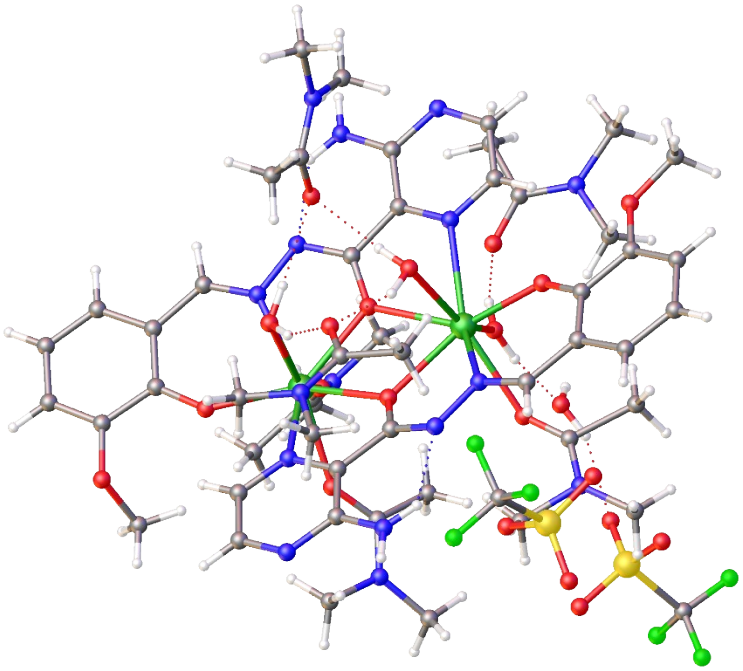

Fig. S4. Hydrogen bonds in **2**.

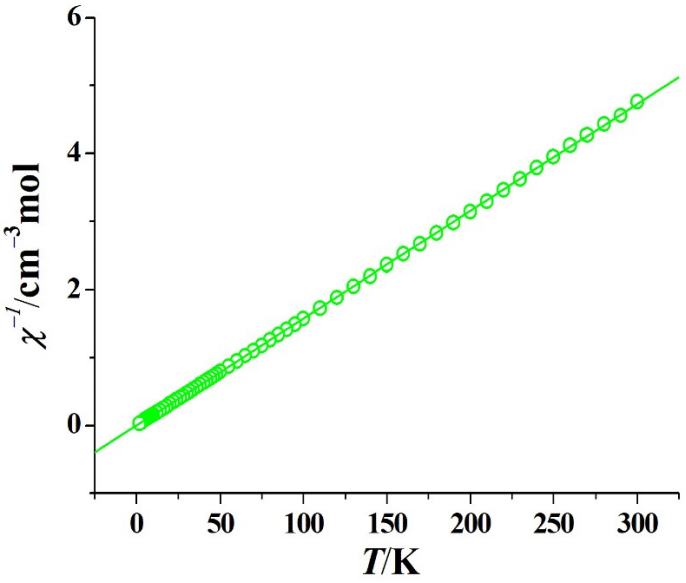

Fig. S5. Plot of $1/\chi_M$ *versus* T of **3** (H_{dc} = 1000 Oe).

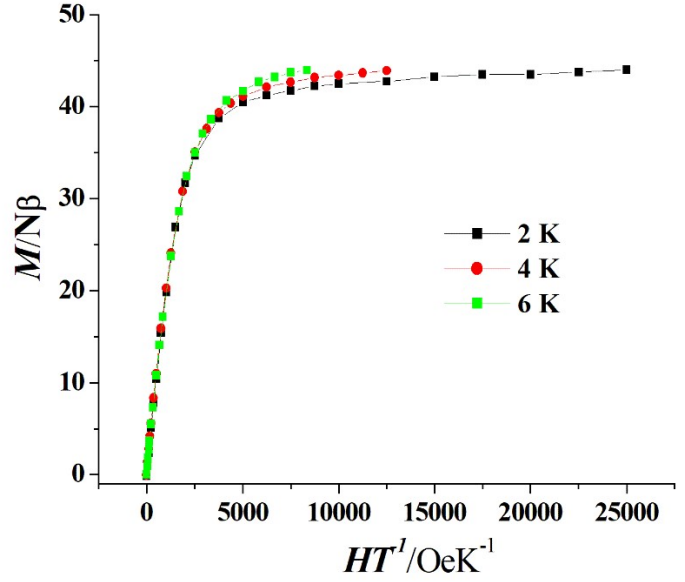

Fig. S6. *M versus H*/*T* plot of **1** at 2, 4 and 6 K.

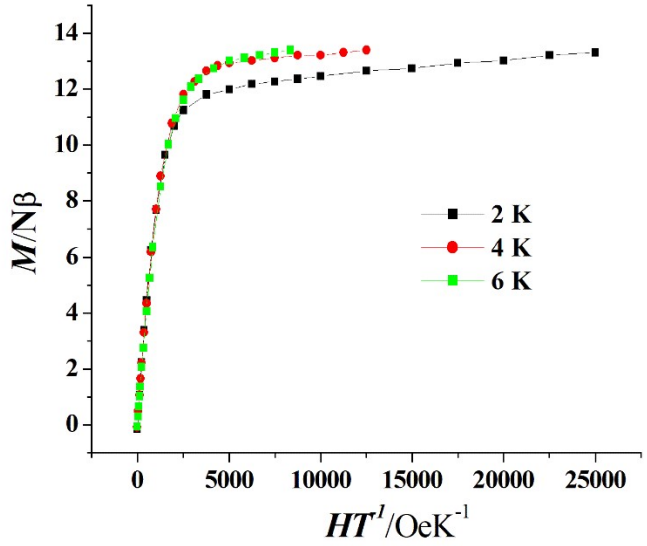

Fig. S7. *M versus H*/*T* plot of **2** at 2, 4 and 6 K.

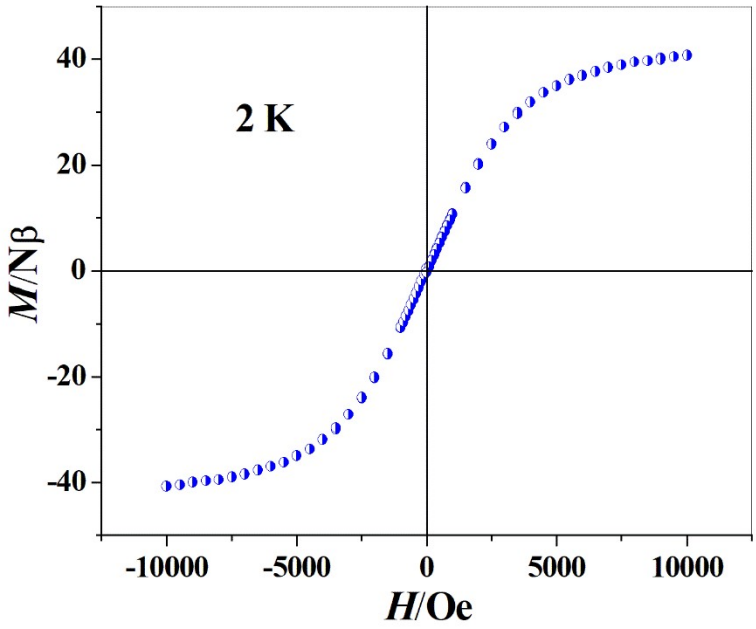

Fig. S8. Hysteresis loop for **1** at 2.0 K.

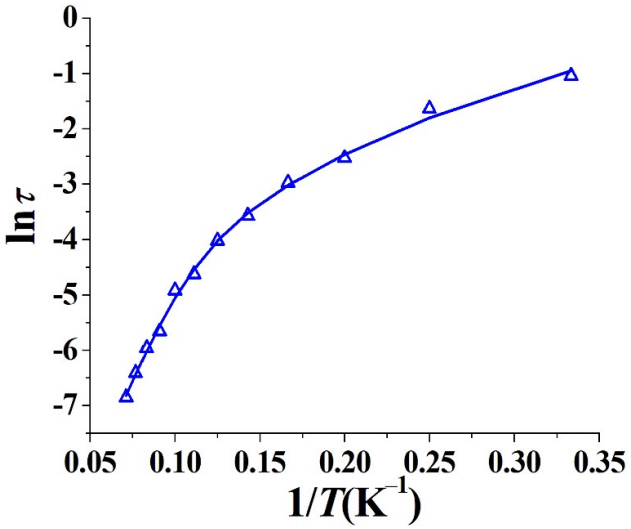

Fig. S9. Plot of ln(τ) *versus* 1/T for **1** (H_{dc} = 1500 Oe), the solid line represents the best fitting with Raman + Orbach.

Table S6. U_{eff}/k and τ_0 values of some zero-field ferromagnetic coupling Dy_2 SMMs.

Structural formula	U_{eff}/k (K, 0 Oe)	τ_0 (s)	Ref.
$Dy_2(hmi)_2(NO_3)_2(MeOH)_2$	56	3×10^{-7}	35
$[Dy_2(hmi)_2(NO_3)_2(MeOH)_2]\cdot MeCN$	71	7×10^{-8}	35
[(Pc)Dy(ooPc)Dy(Pc)]	25.9	2.4×10^{-7}	36
$[Dy_2(L_{Schiff}1)_2(L\text{-pfc})_2(MeOH)_2]$	76.9	1.0×10^{-6}	38
$[Dy_2(L_{Schiff}2)_2(L\text{-pfc})_2(MeOH)_2]$	78.1 180.6	3.5×10^{-8} 3.7×10^{-10}	38
$Dy^{III}_2L_2(acetate)_4(MeOH)_2$	76	1.5×10^{-6}	39
$[Dy_2ovph_2Cl_2(MeOH)_3]_3\cdot MeCN$	150 198	2.3×10^{-8} 7.3×10^{-9}	40
$Dy_2L_2(DMF)_2(NO_3)_2$	58.2	1.0×10^{-5}	42
$Dy_2L_2(DMF)_2(AcO)_2$	59.9	8.0×10^{-6}	42
$Dy_2(l\text{-tfc})_4(chp)_2(MeOH)_2$	180.5	1.5×10^{-11}	55
$Dy_2(d\text{-tfc})_4(chp)_2(MeOH)_2$	181.3	1.5×10^{-11}	55
$[Dy_2(NO_3)_4(L)_2(H_2O)_2]\cdot 2MeCN$	112.0	8.7×10^{-9}	56
$[Dy_2(NO_3)_4(L)_2(H_2O)_2]\cdot 2(NO_3)\cdot DMBD\cdot 2MeOH$	128.2	2.3×10^{-8}	56
$[Dy_2(NO_3)_4(L)_2(TPO)_2]\cdot 2MeCN$	170.0	2.4×10^{-10}	56
$[Dy_2(L')_6(H_2O)_2]\cdot 4MeCN$	255.7	1.7×10^{-10}	56
$[Dy_2(HL)_2Cl_2(H_2O)_3]\cdot 2H_2O\cdot MeCN$	204 103	5.9×10^{-9} 1.8×10^{-8}	57
$[Dy_2(L_{schiff})_2(DMA)_3(H_2O)_3](CF_3SO_3)_2$ $\cdot 3DMA\cdot H_2O$	242.9	1.7×10^{-9}	this work

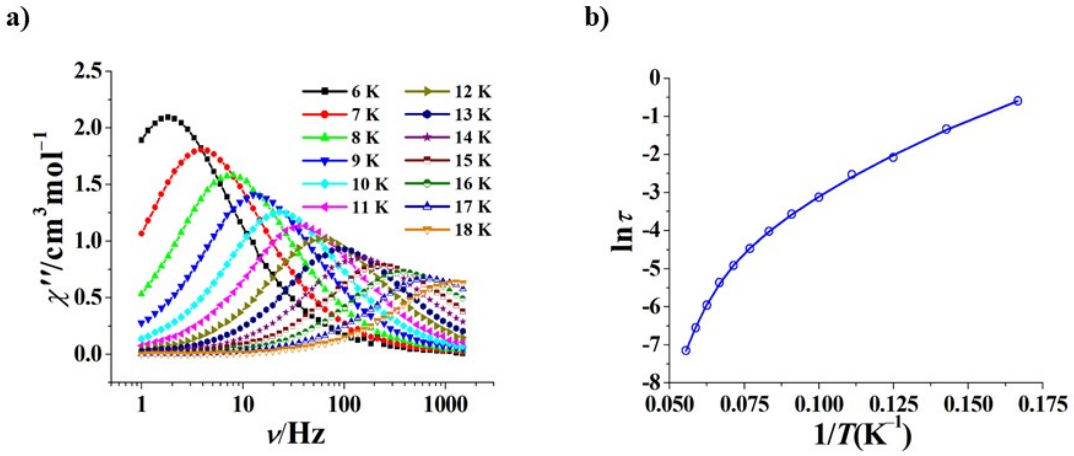

Fig. S10. (a) χ'' *versus* ν curves for **2** (H_{dc} = 1500 Oe); (b) plot of ln(τ) *versus* 1/T for **2** (H_{dc} = 1500 Oe), the solid line represents the best fitting with Raman + Orbach.

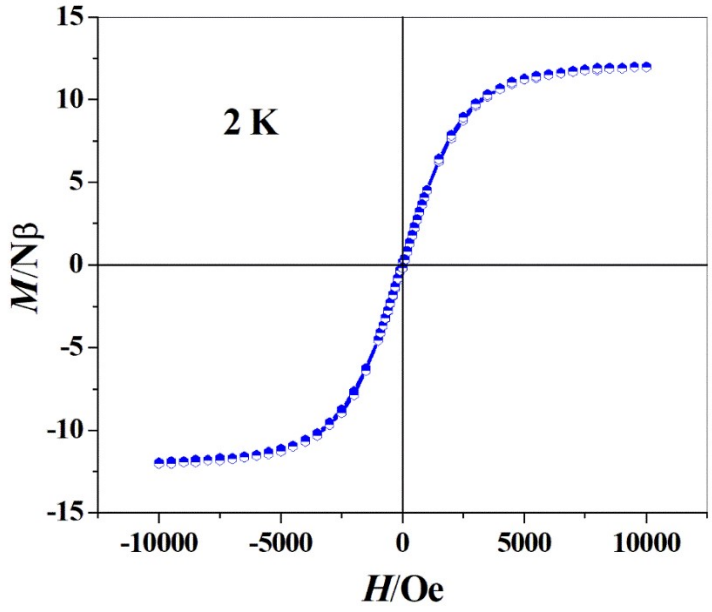

Fig. S11. Hysteresis loop for **2** at 2.0 K.

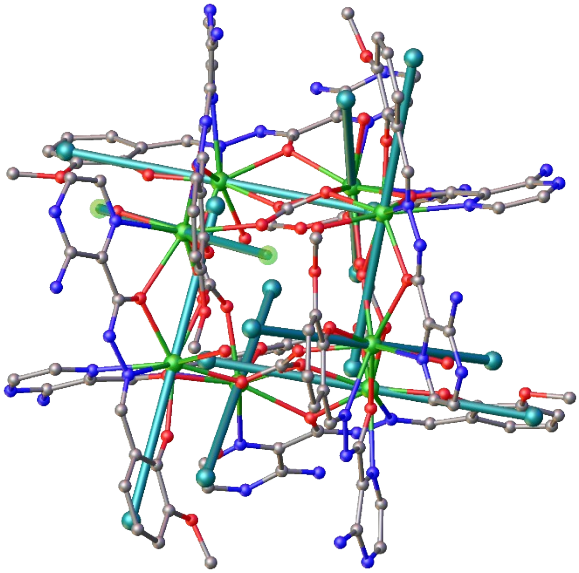

Fig. S12. Magnetic axes of the Dy^{3+} ions in **1** calculated using an electrostatic model.

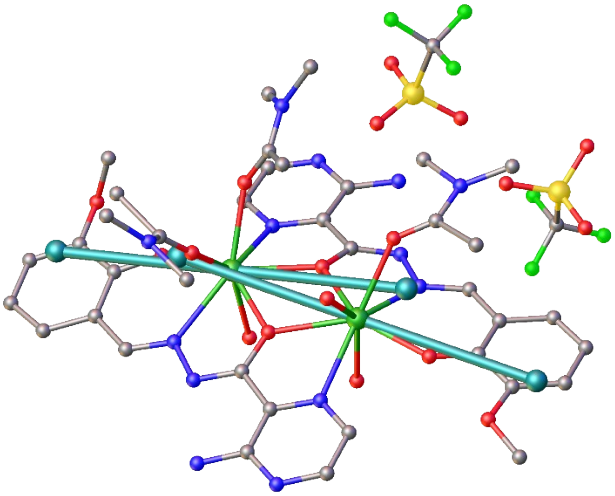

Fig. S13. Magnetic axes of the Dy^{3+} ions in **2** calculated using an electrostatic model.